LASER ABLATION ICP-MS TECHNIQUE AND STANDARDS

The concentrations of PGE and other trace elements (V, Mn, Co, Ni, Cu, Zn and Re) in the Cr-spinel from Siberian meimechite and Uralian ankaramite were determined by LA-ICP-MS at the Research School of Earth Science, at the Australian National University (ANU). This system is comprised of ANU-designed HelEx ablation cell and a Lambda Physik Complex 110 excimer laser (λ=193 nm), linked to an Agilent 7700x quadruple ICP-MS. The analyses were performed using spot sizes that varied between 81 and 105 µm and a laser pulse rate of 8 Hz. Each analysis consisted of 25 s of background measurement followed by 40 s of sample ablation. We used a NIST 610 glass reference material as the primary standard for calculating V, Mn, Ni, Zn, Co, and Re contents with Al content independently measured by electron microprobe analysis employed as the internal standard. CANMET po727 FeS reference material, described in Fonseca (2007) and Barnes et al. (2008), containing ~40 ppm of all PGE, was employed for calibration of Pd, Pt, Rh, Ru, Ir, and Os. Co concentrations, measured by LA-ICP-MS against NIST 610, were used as the internal standard to correct for yield differences in the PGE between samples and the standard. The Co contents of CANMET po727 FeS reference material is 7 ppm (Fonseca, 2007). Standards were analyzed before and after analysis of ~10 unknown samples. Data reduction was performed using Iolite software (Paton et al., 2011) or an in-house Excel spread sheet for the PGE using the relationship described in Longerich et al. (1996) and Sylvester and Eggins (1997).

The homogeneity of CANMET po727 and the stability of the ICP-MS were tested by multiple analyses of the CANMET po727 as an unknown sample. The standard deviations (n=9) for the analyses of the CANMET po727 of all PGE were < 1.1 %. NIST 610, NIST 612 reference materials and an in-house PGE standard at ANU provided by Guilherme Mallmann

were analyzed using the CANMET po727 FeS standard and Co, measured by LA-ICP-MS against NIST 610, as internal standard to assess the data precision and accuracy of the analyses of PGE. Our analyses of the reference materials agree with the values reported in the literature and with working values within 2σ, as reported in Table DR1.

The isotopes used to determine trace elements and PGE concentrations in this study were as follows: ^{49}Ti, ^{51}V, ^{55}Mn, ^{59}Co, ^{61}Ni, ^{65}Cu ^{66}Zn, ^{101}Ru, ^{103}Rh, ^{105}Pd, ^{185}Re, ^{189}Os, ^{191}Os, ^{193}Ir and ^{195}Pt. The isobaric interferences produced by metal argide (MAr^+) were determined from tests conducted on synthetic Ni-sulfide and pure Cu metal (C-430, Fisher Scientific Company), which have very low PGE abundances, with the assumption that the blank-corrected signals of ^{101}Ru and ^{103}Rh in Ni-sulfide and Cu metal are produced only by argide interferences. The production of $^{61}Ni^{40}Ar^+$ and $^{63}Cu^{40}Ar^+$ which interfere with ^{101}Ru and ^{103}Rh, respectively, were small with the range MAr^+/M^+=7.6–9.1 × 10^{-5}. Isobaric interferences were subtracted from the time-integrated signal, based on the measured Cu and Ni count rates in the Cr spinels and the argide production rates. The interference corrections on ^{101}Ru and ^{103}Rh in Cr spinels were < 2 % and <0.1 % respectively. Data were acquired in the time resolved mode to monitor the presence of heterogeneity in the Cr spinel (e.g. PGM inclusions). Micro inclusions were identified from abrupt intensity spikes during the analysis (Fig. DR1), which were excluded from the trace element and PGE concentration calculations.

Barnes, S. J., and Fiorentini, M. L., 2008, Iridium, ruthenium and rhodium in komatiites: Evidence for iridium alloy saturation: Chemical Geology, v. 257, p. 44-58.

Fonseca, R. O. C., Mallmann, G., O'Neill, H. S. C., and Campbell, I. H., 2007, How chalcophile is rhenium? An experimental study of the solubility of Re in sulphide mattes: Earth and Planetary Science Letters, v. 260, p. 537-548.

Longerich, H. P., Jackson, S. E., and Gunther, D., 1996, Laser ablation inductively coupled plasma mass spectrometric transient signal data acquisition and analyte concentration calculation: Journal of Analytical Atomic Spectrometry, v. 11, p. 899-904.

Park, J. W., Campbell, I. H., and Eggins, S. M., 2012, Enrichment of Rh, Ru, Ir and Os in Cr spinels from oxidized magmas: Evidence from the Ambae volcano, Vanuatu: Geochimica et Cosmochimica Acta, v. 78, p. 28-50.

Paton, C., Hellstrom, J., Paul, B., Woodhead, J., and Hergt, J., 2011, Iolite: Freeware for the visualisation and processing of mass spectrometric data: Journal of Analytical Atomic Spectrometry, v. 26, p. 2508-2518.

Sylvester, P. J., and Eggins, S. M., 1997, Analysis of Re, Au, Pd, Pt and Rh in NIST glass certified reference materials and natural basalt glasses by laser ablation ICP-MS: Geostandards Newsletter, v. 21, p. 215-229.

Table DR1. PGE concentrations in reference materials (ppm)

	Ru	Rh	Pd	Os	Ir	Pt
CANMET po727						
#1	36.3	41.5	43.1	47.1	48.2	35.8
#2	37.3	42.2	43.5	48.0	49.6	35.8
#3	36.3	42.1	44.3	46.6	48.6	36.7
#4	36.5	41.4	42.5	47.5	48.4	35.1
#5	36.6	41.8	43.5	47.3	48.7	36.0
#6	36.6	41.8	43.5	47.3	48.7	36.0
#7	36.6	41.8	43.5	47.3	48.7	36.0
#8	36.6	41.8	43.5	47.3	48.7	36.0
#9	36.6	41.8	43.5	47.3	48.7	36.0
average	36.6	41.8	43.4	47.3	48.7	35.9
1σ	0.3	0.2	0.5	0.3	0.4	0.4
NIST610						
#1	0.003	1.39	1.16	0.035	0.071	3.18
#2	0.002	1.42	1.20	0.030	0.067	3.06
#3	0.003	1.40	1.08	0.025	0.065	2.92
#4	0.002	1.38	1.04	0.027	0.064	2.99
#5	0.002	1.43	1.11	0.027	0.061	3.11
#6	0.002	1.40	1.02	0.024	0.058	3.20
#7	0.004	1.44	1.01	0.021	0.059	3.12
#8	0.003	1.42	1.14	0.029	0.067	2.93
#9	0.003	1.45	1.19	0.030	0.069	2.95

average	0.003	1.41	1.10	0.027	0.064	3.05
1σ	0.001	0.02	0.07	0.004	0.004	0.11
NIST610 (Sylvester and Eggins, 1997)		1.31	1.05			3.15
1σ		0.02	0.06			0.08
NIST612						
#1	0.000	1.00	0.92	0.003	0.007	2.40
#2	0.000	0.98	0.85	0.002	0.007	2.34
#3	0.000	0.99	0.86	0.003	0.008	2.32
#4	0.002	1.02	0.83	0.004	0.007	2.40
#5	0.001	0.96	0.87	0.003	0.007	2.59
#6	0.002	0.99	0.77	0.003	0.006	2.24
average	0.001	0.99	0.85	0.003	0.007	2.38
1σ	0.001	0.02	0.05	0.001	0.000	0.12
NIST612 (Sylvester and Eggins, 1997)		0.90	1.09			2.59
1σ		0.01	0.09			0.03
ANU In-house PGE standard						
#1	2503	200	63	244	570	5353
#2	2322	186	58	226	514	4781
#3	2451	198	63	232	532	4918
average	2425	194	61	234	538	5017
1σ	93	8	3	9	29	298
Working values (Park et al., 2012)						
EPMA (n=15)	2340	266				5166
1σ	111	89				332
LA-ICP-MS (n=5)	2362	198	66	239	546	5289
1σ	69	8	2	10	13	193

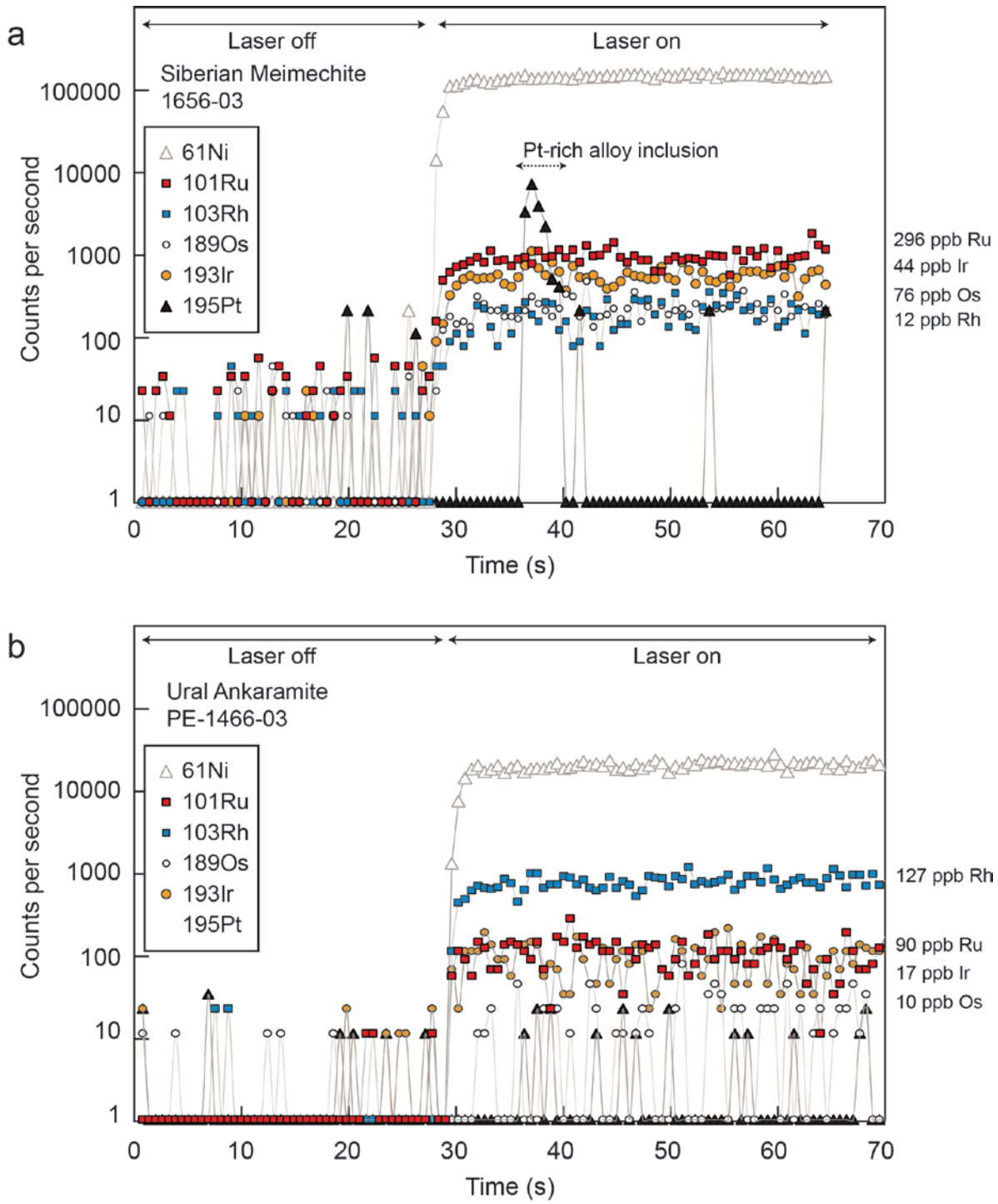

Figure DR1. Representative time resolved LA-ICP-MS spectra of Ni, Rh and IPGE in Cr-spinel from Siberian Meimechite (a) and Uralian Ankaramite (b). A Pt spike in the spectra of the Cr-spinel grain from the Siberian Meimechite represents a Pt-rich inclusion, and is excluded from calculation of PGE contents.

Table DR2. Major (wt%) , trace (ppm) and Platinum-group (ppb) element compositions of bulk rock samples (Siberian meimechite (SM), Ambae picrite (AP) and Uralian ankaramite (UA)

Sample#	**SM (1656)**	**AP (68591)**	**UA (PE-1466)**
wt%			
SiO_2	38.19	47.33	45.43
TiO_2	1.84	0.55	0.17
Al_2O_3	2.82	10.06	6.60
Fe_2O_3	13.21	11.14	9.41
MnO	0.17	0.18	0.20
MgO	33.01	17.75	17.70
CaO	4.36	10.54	16.79
Na_2O	0.13	1.62	0.10
K_2O	0.24	0.92	0.01
P_2O_5	0.21	0.22	0.11
LOI	5.93	-0.17	3.70
CaO/Al_2O_3	1.55	1.05	2.54
ppm			
Sc	9.35	40	41.1
V	53.5	271	139
Cr	825	1187	686
Co	75.8		51.8
Ni	907	413	281
Cu	41.3	93	42.3
Zn	75.8	77	45.7
Ga	4.79	15	4.66
Ge	0.71		1.7
Rb	6.76	17	0.37
Sr	182	488	25.8
Y	6.02	13	3.8
Zr	67.8	39	9.9
Nb	6.74	1.5	0.38
Ba	132	258	10.5
La	16.6	9.6	2.36
Ce	37.7	22.5	4.72
Pr	4.79	2.98	0.60
Nd	19.3	13.7	2.73
Sm	4.02	3.65	0.66
Eu	1.10	1.15	0.20
Gd	3.17	3.39	0.68
Tb	0.39		0.10
Dy	1.93	3.22	0.71
Ho	0.30		0.15
Er	0.67	1.83	0.48
Tm	0.09		0.07
Yb	0.47	1.57	0.46

Lu	0.07	0.07
Hf	2.64	0.27
Pb	3.24	2.15
Th	2.13	0.66
U	0.44	0.31

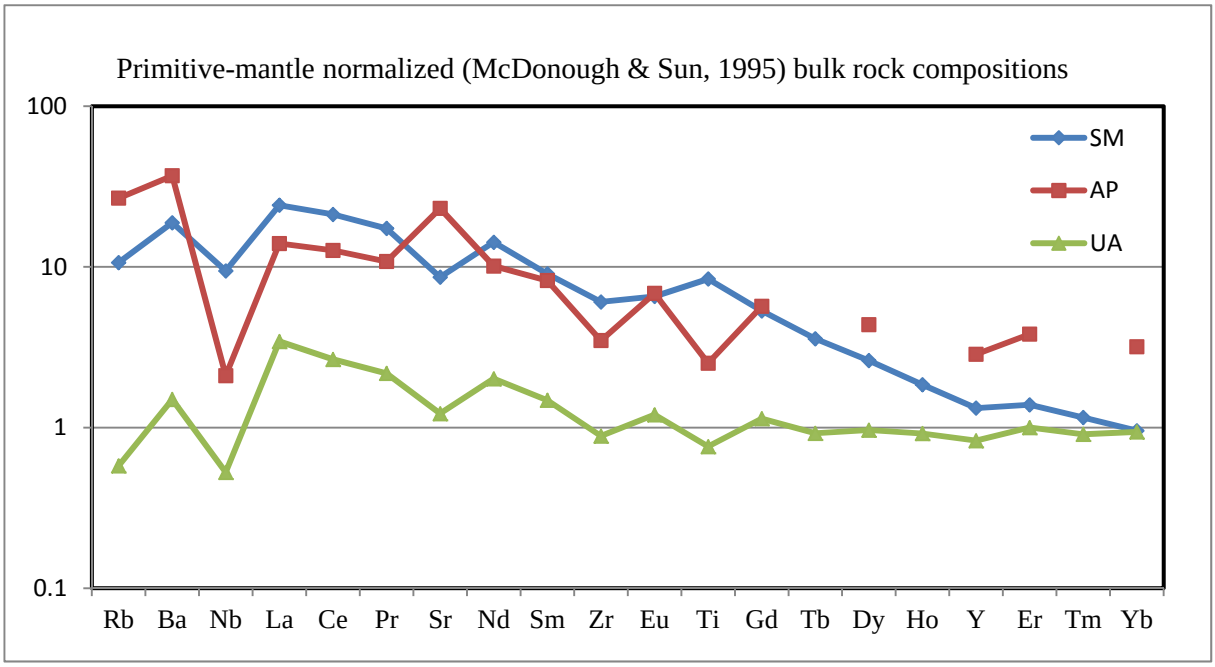

	average (8)	average (3)	
ppb	Mungall et al., 2006	Park et al., 2012	
Ru	2.58	0.11	0.66
Rh	0.45	0.22	0.94
Pd	4.38	2.88	11.9
Ir	1.59	0.18	0.36
Pt	7.83	5.47	23.0
normalized			
Ir	0.496	0.056	0.113
Ru	0.516	0.022	0.132
Rh	0.500	0.240	1.044
Pt	1.103	0.770	3.239
Pd	1.123	0.739	3.051

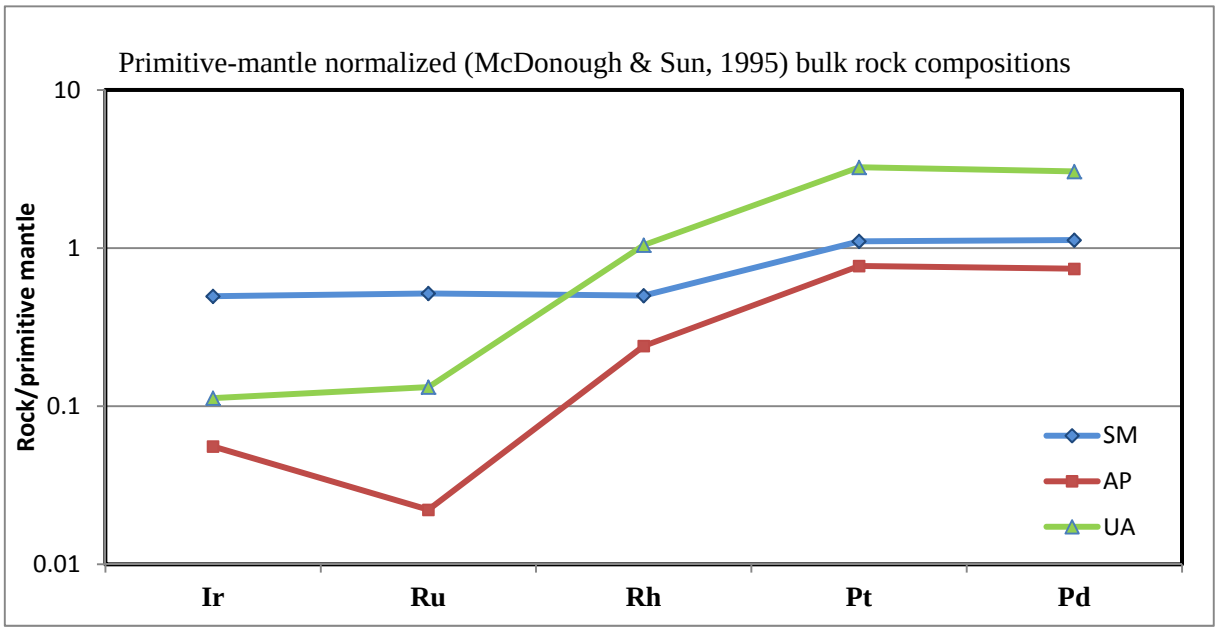

McDonough, W. F., and Sun, S.-s., 1995, The composition of the Earth: Chemical Geology, v. 120, no. 3-4, p. 223-253.

Mungall, J. E., Hanley, J. J., Arndt, N. T., and Debecdelievre, A., 2006, Evidence from meimechites and other low-degree mantle melts for redox controls on mantle-crust fractionation of platinum-group elements: Proceedings of the National Academy of Sciences of the United States of America, v. 103, no. 34, p. 12695-12700.

Park, J. W., Campbell, I. H., and Eggins, S. M., 2012, Enrichment of Rh, Ru, Ir and Os in Cr spinels from oxidized magmas: Evidence from the Ambae volcano, Vanuatu: Geochimica Et Cosmochimica Acta, v. 78, p. 28-50.

Table DR3. Major (wt%) , trace (ppm) and Platinum-group (ppb) element compositions of individual Cr-spinel phenocrysts (Siberian meimechite (SM) and Uralian ankaramite (UA)

Analysis No.		SM(1656)-01	SM(1656)-02	SM(1656)-03	SM(1656)-04	SM(1656)-05	UA(PE-1466)-01	UA(PE-1466)-02	UA(PE-1466)-03	UA(PE-1466)-04	UA(PE-1466)-05	UA(PE-1466)-06	UA(PE-1466)-07	UA(PE-1466)-08
Remarks			Pt spike excluded	Pt-Ir spike excluded										
Cr_2O_3	wt%	44.2	39.3	41.1	48.2	43.3	63.7	64.0	63.7	64.4	64.1	64.9	64.2	63.9
Al_2O_3	wt%	6.3	5.9	6.3	6.2	6.0	5.0	4.7	4.7	5.0	5.0	4.6	4.7	5.1
TiO_2	wt%	5.0	6.6	5.8	3.9	5.1	0.16	0.16	0.18	0.16	0.15	0.16	0.15	0.17
FeO	wt%	20.1	20.7	20.7	18.4	18.9	14.5	14.6	15.2	14.5	14.6	14.4	14.7	14.7
Fe_2O_3	wt%	12.4	15.0	14.0	10.7	14.0	5.3	5.2	5.2	5.1	4.9	4.7	4.9	4.9
MgO	wt%	11.1	11.6	11.1	11.5	11.9	12.2	12.1	11.7	12.4	12.2	12.3	12.0	12.1
total	wt%	99.1	99.1	99.0	98.9	99.1	100.9	100.8	100.8	101.6	100.9	101.1	100.6	100.9
Fe^{2+}/Fe^{3+}		1.80	1.53	1.64	1.92	1.50	3.03	3.12	3.24	3.16	3.29	3.39	3.36	3.34
$Fe^{3+}/\sum Fe$		0.36	0.40	0.38	0.34	0.40	0.25	0.24	0.24	0.24	0.23	0.23	0.23	0.23
$Mg/(Mg+Fe^{2+})$		0.50	0.50	0.49	0.53	0.53	0.60	0.60	0.58	0.60	0.60	0.60	0.59	0.59
Cr/(Cr+Al)		0.82	0.82	0.81	0.84	0.83	0.89	0.90	0.90	0.90	0.90	0.90	0.90	0.89
$Cr/\sum R^{3+}$		0.68	0.63	0.64	0.71	0.66	0.84	0.84	0.84	0.84	0.84	0.85	0.85	0.84
$Fe^{3+}/\sum R^{3+}$		0.18	0.23	0.21	0.15	0.20	0.07	0.07	0.07	0.06	0.06	0.06	0.06	0.06
Si	ppm	167	189	176	166	155	1423	1498	1492	6390	1395	1520	1393	1459
Sc	ppm	11	16	11	10	11	9	10	11	10	9	10	9	9
Ti	ppm	31174	32963	32271	22964	29113	935	974	1072	987	926	933	915	995
V	ppm	673	737	690	447	651	931	961	1011	874	888	961	927	969
Mn	ppm	1571	1661	1753	1433	1425	1925	2082	2205	1815	1963	2164	1996	2016
Co	ppm	208	216	224	192	201	245	266	285	232	253	277	255	259
Ni	ppm	1562	1756	1507	1426	1447	559	597	612	547	553	592	550	567
Cu	ppm	30	39	43	23	20	8	9	9	8	8	9	9	9
Zn	ppm	372	353	440	317	336	408	444	468	381	414	451	432	442
Ru	ppb	232	254	296	198	233	33	65	90	79	34	55	75	66
Rh	ppb	12	12	12	8	12	55	85	127	75	56	68	65	78
Pd	ppb	<3	<3	<3	<3	<3	<1	<1	<1	<1	<1	<1	<1	<1
Re	ppb	<2	<2	<2	<2	<2	n.a.	n.a.	n.a.	n.a.	n.a.	n.a.	n.a.	n.a.
Os	ppb	83	89	76	113	92	<2	6	10	4	<2	6	5	5
Ir	ppb	50	56	44	58	47	3	20	17	8	3	4	8	6
Pt	ppb	<1	<1	<1	<1	<1	<2	<2	<2	<2	<2	<2	<2	<2
OsN		24.5	26.1	22.2	33.4	27.0		1.8	2.9	1.2		1.7	1.4	1.3
IrN		15.7	17.6	13.7	18.3	14.7	1.0	6.2	5.2	2.4	1.0	1.2	2.5	2.0
RuN		46.4	50.9	59.2	39.7	46.6	6.6	13.0	18.0	15.8	6.8	11.0	15.0	13.2
RhN		13.7	13.0	13.9	9.3	13.4	61.6	93.9	141.2	83.0	62.0	75.7	72.1	87.0

Table DR4. Comparison of measured PGE concentrations with model alloy solubilities

Model		SM (oxidized)[1]	SM (reduced)[2]	AP	UA
	T (^{o}C)	1450	1450	1170	1250
	XFe (alloy; mole fraction)	-	-	0.17	0.4
Kessel et al. (2001)	ΔFMQ (log_{10} units) [3]	-	-	2.21	-0.54
Ballhaus et al. (1991)	ΔFMQ (log_{10} units) [4]	2.62	1 (estimate)	2.65	-
Mungall and Brenan (2014)	log fS2	-	-	-	0.47
	Pt (ppb, meas)	7.83	7.83	5.47	23
Mungall and Brenan (2014)	[Pt] (ppb) [5]	490	88	14.3	2.08
Mungall and Brenan (2014)	[Pt] corrected for aPt (ppb) [6]	240	26	7.83	0.19
Mungall and Brenan (2014)	[Pt] corrected for fS2 (ppb) [7]	240	26	7.83	23.6
	Ir (ppb, meas)	1.59	1.59	0.18	0.36
Mungall and Brenan (2014)	[Ir] (ppb) [5]	71.3	4.35	0.3	0.012
Mungall and Brenan (2014)	[Ir] corrected for alloy (ppb) [8]	26.4	1.61	0.11	0.004
Mungall and Brenan (2014)	[Ir] corrected for fS2 (ppb) [7]	26.4	1.61	0.11	59

[1] calculations done at fO2 estimated from mineral compositions

[2] calculations done at arbitrarily chosen fO2 1 log unit above FMQ

[3] fO2 calculated from PtFe alloy composition (Kessel et al., 2001)

[4] fO2 calculated from olivine-spinel pairs (Ballhaus et al., 1991)

[5] estimated solubility of pure metal, ppb (Mungall and Brenan, 2014)

[6] metal solubility corrected for activity in alloy phase, ppb (Kessel et al., 2001)

[7] alloy solubility assuming formation of MS melt complexes, ppb (Mungall et al., 2014)

[8] metal solubility corrected assuming ideal mixing in multicomponent alloy

Ballhaus, C., Berry, R. F., and Green, D. H., 1991, High pressure experimental calibration of the olivine-

orthopyroxene-spinel oxygen geobarometer: implications for the oxidation state of the upper mantle: Contributions to Mineralogy and Petrology, v. 107, p. 27-40.
Kessel, R., Beckett, J. R., and Stolper, E. M., 2001, Thermodynamic properties of the Pt-Fe system: American Mineralogist, v. 86, no. 9, p. 1003-1014.
Mungall, J. E., and Brenan, J. M., 2014, Partitioning of platinum-group elements and Au between sulfide liquid and basalt and the origins of mantle-crust fractionation of the chalcophile elements: Geochimica Et Cosmochimica Acta, v. 125, p. 265-289.

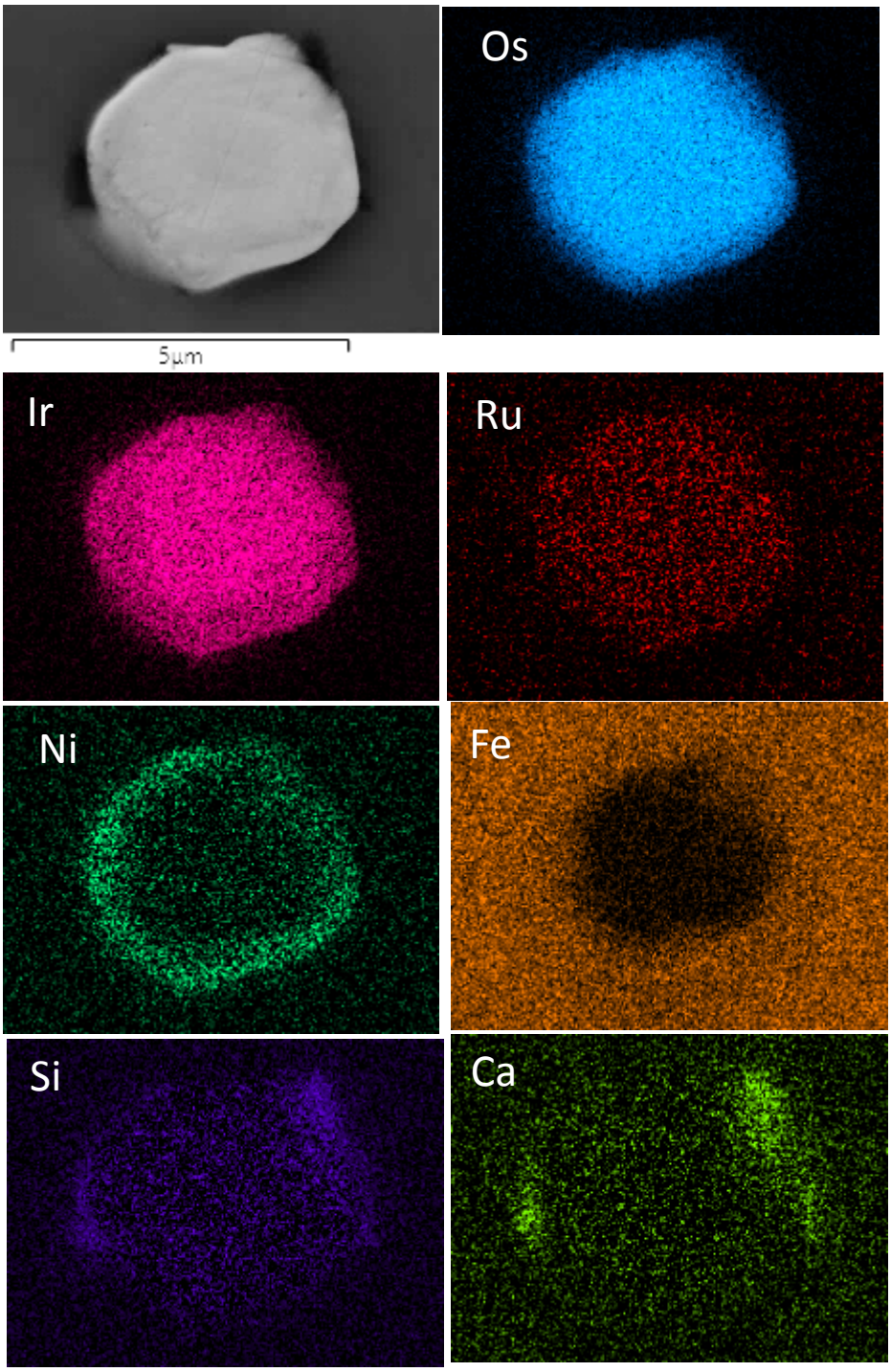

Figure DR2A. Back-scattered electron image and X-ray element maps of Os-Ir inclusion in Cr-spinel phenocryst from the Siberian meimechite (Figs. 2 A, B)

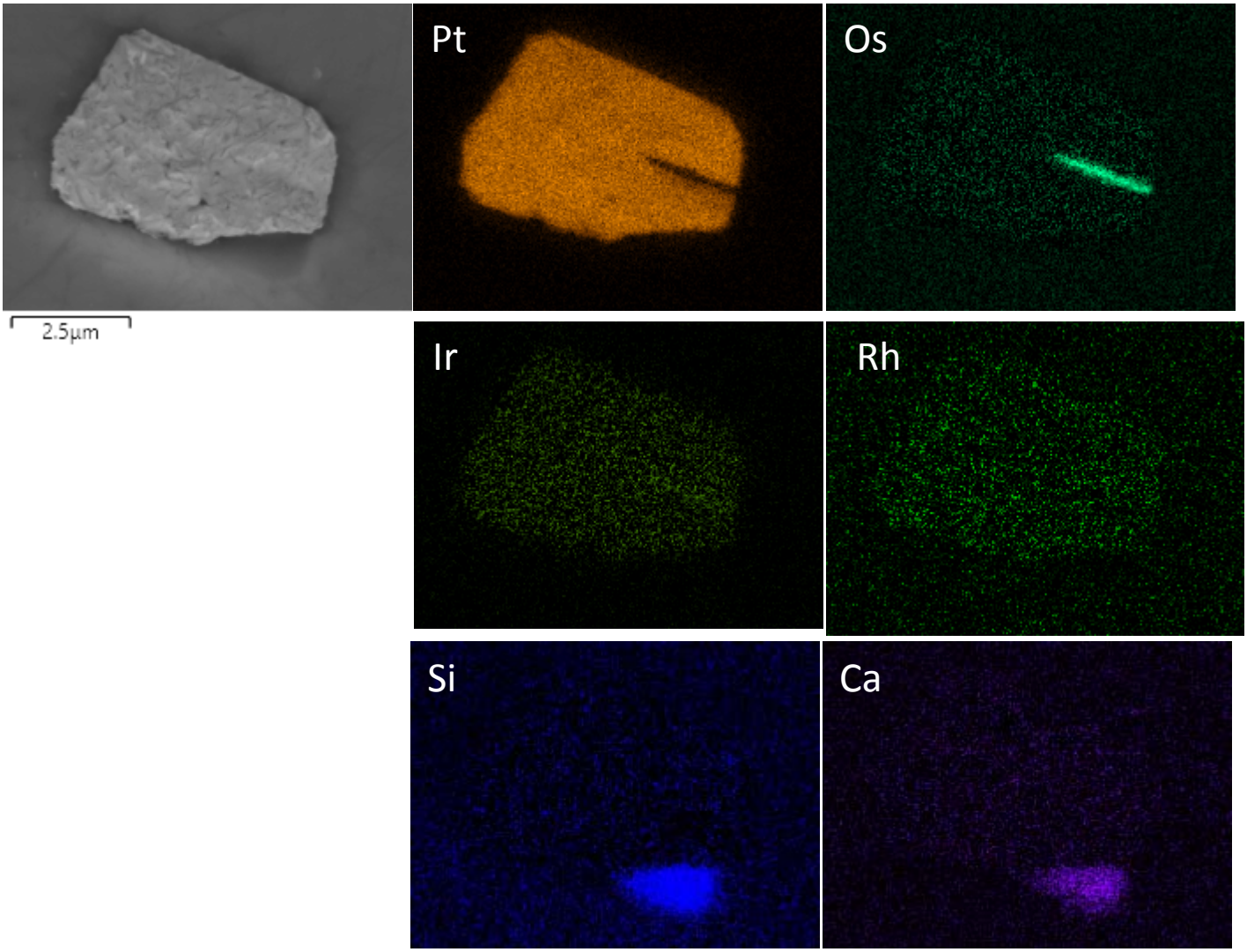

Figure DR2B. Back-scattered electron image and X-ray element maps of Pt-Fe alloy inclusion in Cr-spinel phenocryst from the Ambae picrite (Figs. 2 C, D)

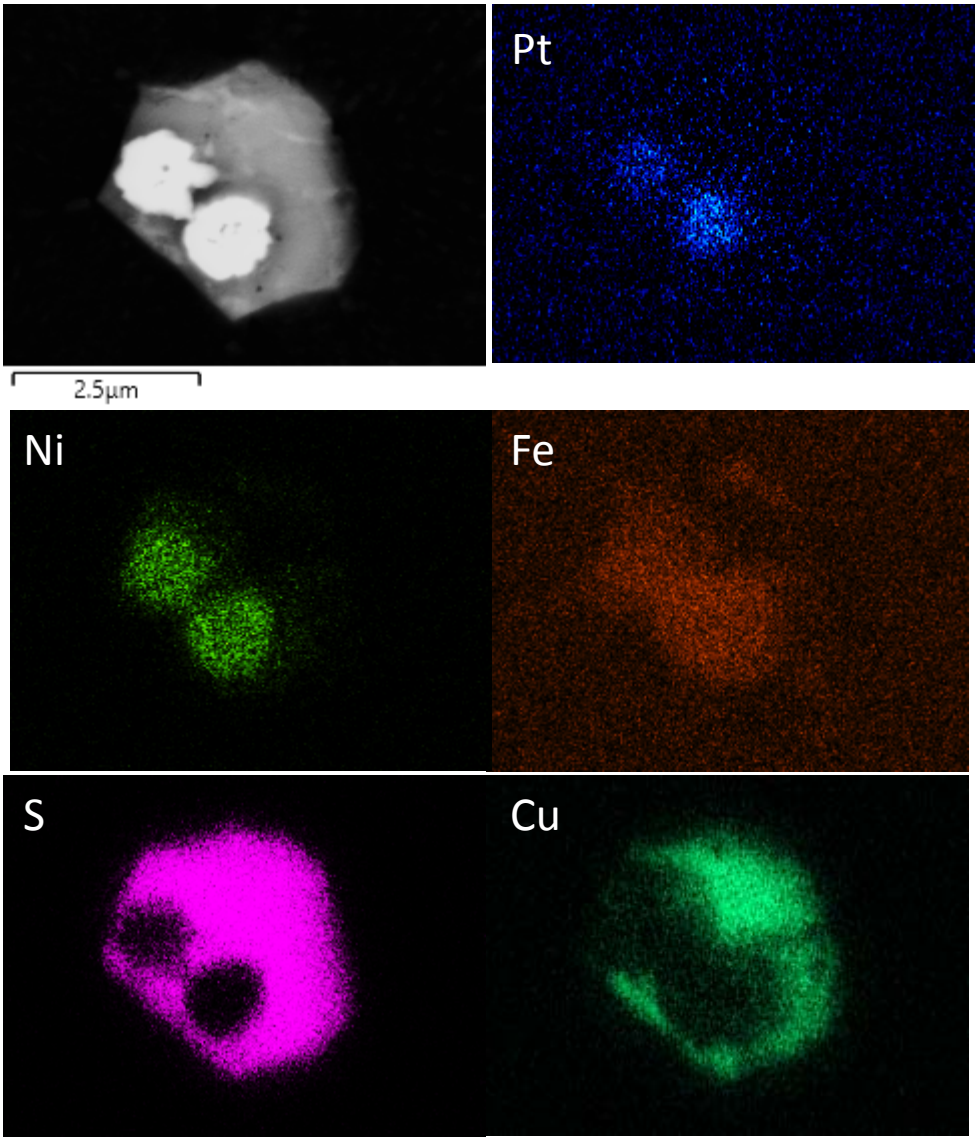

Figure DR2C. Back-scattered electron image and X-ray element maps of Pt-bearing Fe-Ni alloys in the Cu-sulfide inclusion in Cr-spinel phenocryst from the Uralian ankaramite (Fig. 2H)

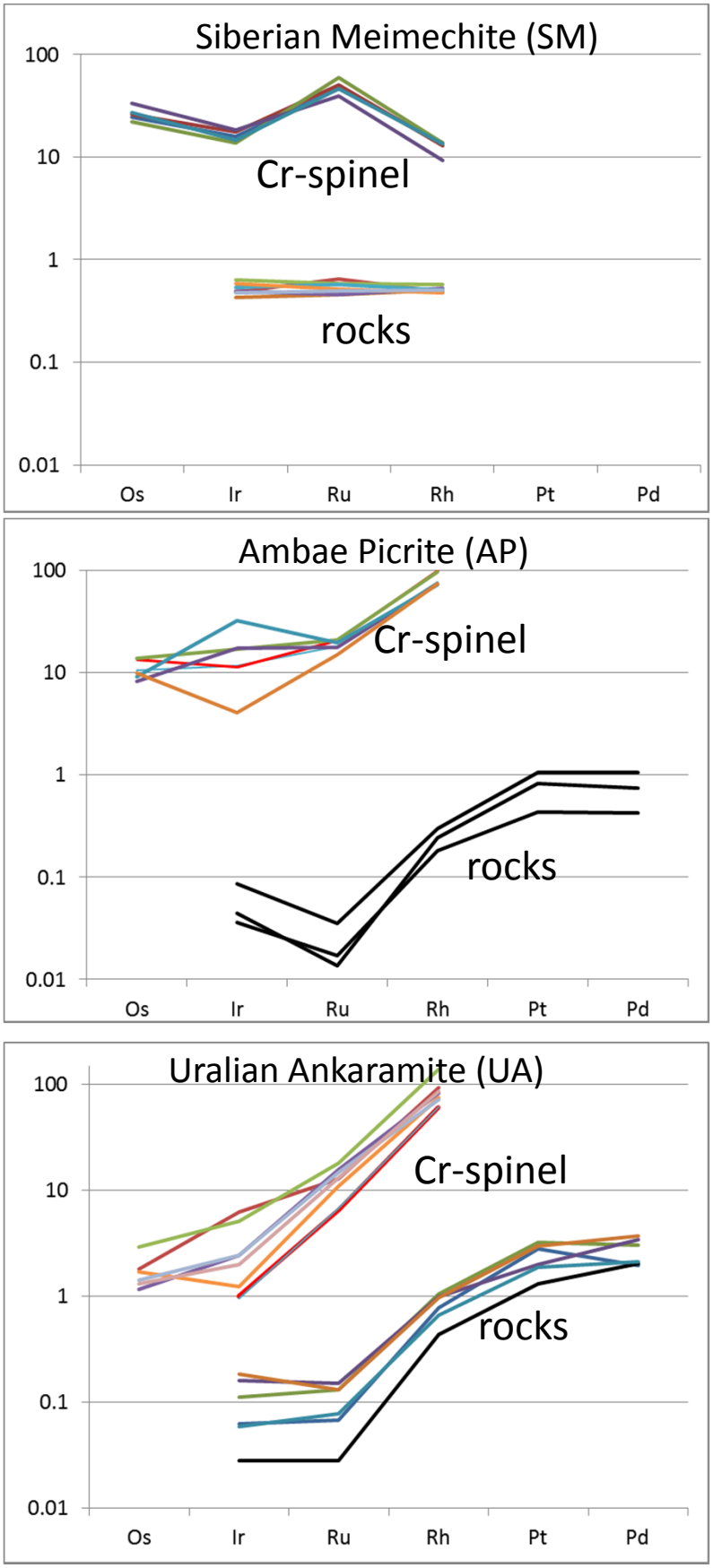

Figure DR3. Mantle-normalized (after McDonough and Sun, 1995) PGE compositions of rocks and Cr-spinel phenocrysts. The data for the Ambae picrites and Siberian meimechites (rocks only) are from Park et al., 2012 and Mungall et al., 2006, respectively.